BackScatter-Assisted Indoor mmWave Communications with Directional Beam at User

BackScatter-assisted Indoor mmWave Communications with Directional Beam at User

Nancy Varshney*, Reza Ghazalian†, Riku Jäntti†, and Swades De*
* Department of Electrical Engineering and Bharti School of Telecommunication
Indian Institute of Technology Delhi, New Delhi 110016, India
† Department of Communications and Networking, Aalto University, 02150 Espoo, Finland
E-mail: Nancy.Varshney@dbst.iitd.ac.in, {reza.ghazalian, riku.jantti}@aalto.fi, and swadesd@ee.iitd.ac.in

***Abstract*—Owing to large spectrum availability, millimeter wave (mmWave) communications are being proposed for 5th generation and beyond networks. However, the mmWaves are easily obstructed by objects, resulting in complete link blockage, which is more common in indoor communication. In this study, we propose to use the existing infrastructure of passive backscatter devices to establish links between the access point and a blocked legacy mobile user, with uncertain coordinates, in an indoor mmWave communication system. We set up backscatter devices in retro-reflective mode for the user to estimate the direction of arrival from them. To estimate the angles, we propose an estimator and derive its Cramer-Rao lower bound. Furthermore, while accounting for the antenna array configuration at both the user and the backscatter devices, we maximize the rate support at the user by optimizing the backscatter device reflection coefficient and the user's steering angle. The simulation results show that, by exploiting the backscatter devices already present in the environment with a sufficient number of antenna elements at the user, higher capacity is achieved as compared to that achieved by using a fixed re-configurable intelligent surface.**

***Index Terms*—Angle of arrival, backscatter devices, clustering, reflection coefficient, steering.**

I. Introduction

Millimeter wave (mmWave) communication system have been proposed by 5th generation and beyond networks for providing high data rates. mmWave communication has higher directivity because of deployment of antenna arrays and offer large bandwidth enabling data rates on order of gigabits [1]. Indoor wireless communication is expected to improve as well with the use of mmWave communications. Nonetheless, mmWave signals are easily obstructed by objects such as walls, metals, and so on. A large number of access points (APs) must be deployed to provide complete coverage in indoor mmWave communications. Since, the cost of deploying a dense network at mmWave is quite large thus, increasing the number of APs beyond a certain limit is not feasible. To this end, several studies have investigated the use of low cost passive reconfigurable intelligent surfaces (RISs) to improve indoor coverage and proposed various joint transmitter and RIS beamforming designs to maximize spectral and energy efficiency of the system [2], [3].

Another contemporary technology is backscatter communication that will play a crucial role in the development of smart indoor environments in near future by connecting low-power wireless devices. By leveraging the existing backscatter infrastructure, the performance of an indoor mmWave communication system can be improved without incurring any extra capital cost. The tags, when in idle mode, can be used to create a additional line-of-sight (LoS) link at mmWave range between the AP and the legacy user. The authors in [4] suggested employing backscatter devices with multiple-input-multiple-output (MIMO) systems to create an artificial rich scattering environment. The results demonstrated enhanced system performance. However, the investigation was performed at sub-6 GHz with single antenna tags, and transmitters and receivers employed digital beamforming with an equivalent number of RF chains as the number of antenna elements. Digital beamforming is not preferred at the mmWave range, especially at user end, because RF chains are power-hungry devices.

Therefore, towards achieving a low cost and low power adaptive backscatter environment for high data rate indoor communication at mmWaves, we consider the AP as well as the users are equipped with a single RF chain connected with the respective antenna array. All devices at mmWave range, including AP, user, and tags, have several antenna elements to combat high attenuation. Authors in [5] reported the use of multi-antenna tags for backscatter communication at mmWave range. A multi-antenna tag can be utilized to direct the incoming signal from the AP to the legacy user by optimizing the coefficients of the reflecting elements. It is noteworthy that a tag in this scenario just reflects the incoming signal; it does not modulate the incoming data in any way thereby creating a virtual path between the AP and user. Consequently, in this work the multi-antenna tags-assisted mmWave communication system is analogous to distributed RIS-assisted mmWave communication system, i.e, the the multi-antenna backscatter devices operate same as small sized RISs distributed over an area.

Furthermore, similar to RIS, the reflection coefficient vector of multi-antenna tags can be optimized using channel state information (CSI) or angular information estimated during beam training [6]. However, it is computationally difficult to estimate the exact CSI of the cascaded channel between the AP, tag and user. Therefore, we use the angular information to optimize the weights at the tags. For this, we need to estimate angle ϕ between a tag and the user and the angle ϕ' between

the AP and a tag. The traditional sub-spaced based algorithms, such as multiple signal classification (MUSIC) and estimation of signal parameters via rotational invariance (ESPRIT), and others are incapable of estimating the angle with a single RF chain [7]. This is because these algorithms require the same number of RF chains as the number of antenna elements to determine spatial correlation. The works in [8] and [9] used the retro-reflective property for localization and beamforming in backscatter communication at mmWave range. When an antenna array is configured in retro-reflective mode it reflects the signal back in the same direction. Therefore, ϕ and ϕ' can be estimated independently at user and AP end, respectively, without depending on the cascaded channel information. And this information can be exchanged with tags over sub-6 GHz for optimizing the tags' coefficients. Moreover, the size of the antenna array connected to a single RF chain at the AP or/and user affects the performance of backscatter assisted communications. This is so because with increasing array size, the error in angle estimation decreases while the number of effective tags falling within a beam reduces. Therefore, it is interesting to investigate system performance at mmWaves in relation to antenna array size. The overall contributions are:

- A novel backscatter-assisted indoor mmWave communication system is proposed and investigated, in which AP and user are each equipped with a single RF chain connected to an antenna array, and each passive tag has multiple reflecting elements.
- For user with unknown coordinates, a maximum likelihood (ML) based angle-of-arrival (AoA) estimator is proposed to estimate the direction of arriving signals from all the tags that are configured in retro-reflective antenna mode. The initial AoA estimate is obtained using orthogonal matching pursuit (OMP) algorithm. Thereafter, the tags' reflection coefficients are optimized based on the estimated angles. Furthermore, the Cramer-Rao bound of the estimator is also derived.
- Different methods for determining optimal beam steering direction at the user are also investigated. Additionally, the performance of backscatter-assisted indoor mmWave communication system is compared to that of a single RIS-assisted indoor mmWave communication system for different antenna array sizes at the user.

II. System Model

Consider a wideband system having an AP, a mobile user, and T backscatter tags in a 2-dimensional scenario, as shown in Fig. 1. The direct line-of-sight (LoS) path between the AP and the mobile user is completely blocked by a wall. The AP and user are equipped with a broadside uniform linear antenna array (ULA), having N_{AP} and N_U antenna, respectively, placed along the y-axis. Both AP and user are equipped with a single RF chain. The tags are distributed homogeneously with density λ tags/m^2. Also, as the tags are passive devices, each tag is assumed to have N_T reflecting elements placed along y-axis.

Let the wideband channel of bandwidth B be divided into N_c subcarriers. Let the AP transmits signal $x[n]$ of power P through its ULA steered at an angle Ω_{AP}, where $n = \{1, \ldots, N_c\}$. Then the signal received at the user via i^{th} tag over n^{th} subcarrier is

$$y_i[n] = \boldsymbol{b}^H(\Omega_U)\boldsymbol{H}_i\boldsymbol{\Gamma}_i[n]\boldsymbol{G}_i\boldsymbol{b}(\Omega_{AP})[n]x[n] + z_i[n] \quad (1)$$

where $\boldsymbol{G}_i[n]$ is the downlink channel from AP to i^{th} tag and $\boldsymbol{H}_i[n]$ is the downlink channel from i^{th} tag to user over n^{th} subcarrier. $\boldsymbol{b}(\Omega_{AP})$ and $\boldsymbol{b}(\Omega_U)$ are analog steering vector of AP steered at an angle Ω_{AP} and analog combiner of user steered at an angle Ω_U, respectively. $z_i[n]$ is noise variable with distribution $\mathcal{N}(0, \sigma^2)$. $\boldsymbol{\Gamma}_i \in \mathbb{C}^{N_T \times N_T}$ denotes the reflection coefficient matrix of i^{th} tag which is of the form

$$\boldsymbol{\Gamma_i} = \text{diag}\{\zeta e^{j\nu_{i,1}}, \ldots, \zeta e^{j\nu_{i,N_T}}\}. \quad (2)$$

In (2), ζ represents the amplitude attenuation and $\nu_{i,m}$ represents the phase shift of the m^{th} reflecting element of i^{th} tag. The array steering vector of a ULA having N antennas at the angle Ω is given as

$$\mathbf{b}(\Omega) = \frac{1}{\sqrt{N}}\left[1, e^{-j\frac{2\pi d'}{\lambda_c}\sin\Omega} \ldots, e^{-j\frac{2\pi d'}{\lambda_c}(N-1)\sin\Omega}\right]^T \in \mathbb{C}^{N\times 1} \quad (3)$$

where λ_c is the carrier wavelength and $d' = \lambda_c/2$ is the inter element spacing. Considering only LoS path, the mmWave channel over a subcarrier between AP and i^{th} tag, and between i^{th} tag and user, respectively, are

$$\begin{aligned}\boldsymbol{G}_i[n] &= \sqrt{N_T N_{AP}}\, g_i q(n, \tau_g)\mathbf{a}_{\text{R}}(\phi_{i,g})\mathbf{a}_{\text{T}}^H(\theta_{i,g}) \in \mathbb{C}^{N_T \times N_{AP}} \\ \boldsymbol{H}_i[n] &= \sqrt{N_T N_U}\, h_i q(n, \tau_h)\mathbf{a}_{\text{R}}(\phi_{i,h})\mathbf{a}_{\text{T}}^H(\theta_{i,h}) \in \mathbb{C}^{N_U \times N_T}\end{aligned} \quad (4)$$

where g_i and h_i are Ricean distributed small scale fading gain of AP-i^{th} tag channel and i^{th} tag-user channel, respectively. $q(n, \tau) = e^{-j2\pi(n-1)\Delta f\tau}$ is phase shift at n^{th} subcarrier with delay τ. τ_g and τ_h are path delay of AP-i^{th} tag channel and i^{th} tag-user channel, respectively. Δf is the subcarrier bandwidth, $\phi_{i,g}$ is AoA at i^{th} tag from AP, $\theta_{i,g}$ is angle-of-departure (AoD) of AP to i^{th} tag, $\phi_{i,h}$ is the AoA at user from i^{th} tag, and $\theta_{i,h}$ is AoD of i^{th} tag. Here, $\mathbf{a}_{\text{T}}(\cdot)$ and $\mathbf{a}_{\text{R}}(\cdot)$ are

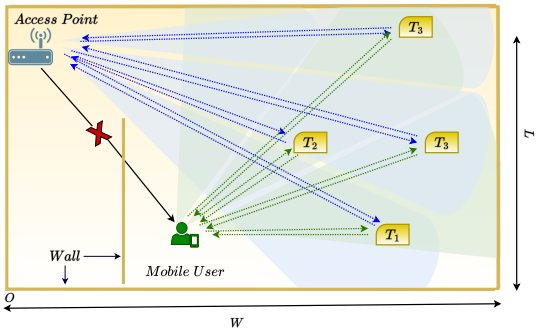

Figure 1: Illustration of backscatter-assisted mmWave communications system model with tags configured in retro-reflective mode.

respectively transmit and receive array manifold. The array manifold of a ULA having N antennas at an angle ω is as

$$\mathbf{a}(\omega)=\frac{1}{\sqrt{N}}\left[1, e^{-j\frac{2\pi d'}{\lambda_c}\sin(\omega)}\ldots, e^{-j\frac{2\pi d'}{\lambda_c}(N-1)\sin(\omega)}\right]^T \mathbb{C}^{N\times 1}. \tag{5}$$

Note, AoAs' and AoDs' are measured with respect to the broadside of an ULA. Assuming that the reflecting surface of all the tags face the user and the plane of reflecting surface of tags lie in the plane of user's ULA, we have $\phi_{i,h}=\theta_{i,h}=\phi_i$. Similarly, $\phi_{i,g}=\theta_{i,g}=\phi'_i$. Therefore, the signal received at user from T tags over a subcarrier n is

$$\begin{aligned} y[n]=&\boldsymbol{b}^H(\Omega_U)\sum_{i=1}^{T}\boldsymbol{H}_i[n]\boldsymbol{\Gamma_i}\boldsymbol{G}_i[n]\boldsymbol{b}(\Omega_{AP})x[n]+z[n]\\ =&N_T\sqrt{N_{AP}N_U}\boldsymbol{b}^H(\Omega_U)\left(\sum_{i=1}^{T}h_i g_i q(n,\tau_h)q(n,\tau_g)\right.\\ &\left.\mathbf{a}_{\mathrm{R}}(\phi_i)\mathbf{a}_{\mathrm{T}}^H(\phi_i)\boldsymbol{\Gamma_i}\mathbf{a}_{\mathrm{R}}(\phi'_i)\mathbf{a}_{\mathrm{T}}^H(\phi'_i)\boldsymbol{b}(\Omega_{AP})x[n]\right)+z[n] \end{aligned} \tag{6}$$

Since the beams of the tags do not point to each other so the signal bouncing from tag to another can be considered to be very weak and is thus ignored. Therefore, the achievable downlink rate over N_c subcarriers is

$$R=\sum_{n=1}^{N_c}\frac{B}{N_c}\log_2\left(1+\frac{y[n]y^H[n]}{\sigma^2}\right). \tag{7}$$

In this paper, we assume that the user is mobile. Hence, its relative location from the tags is unknown. Therefore, to establish a link between the AP and the user we need to optimize $\{\boldsymbol{\Gamma}_i\}_{\forall i}$, Ω_{AP} and Ω_U. In a given indoor communication scenario, the location of AP and tags are fixed. Since the AP has high processing capabilities therefore, for analysis simplicity we assume that the channel $\mathbf{G}_i$ is known a prior. Thus, $\{\phi'_i\}_{\forall i}$ for all $i=\{1,\ldots,T\}$ and Ω_{AP}, are known perfectly at the AP and tags. Hence, in this paper we only estimate $\{\phi_i\}_{\forall i}$ and based on that optimize Ω_U and $\{\boldsymbol{\Gamma}_i\}_{\forall i}$.

III. Link Establishment Procedure

The complete link establishment process is divided into three phases. In first phase, denoted by angle estimation phase, all the tags are configured in retro reflective mode. Therefore, an incident signal get reflected in the same direction. Further, a user equipped with a ULA having N_U antenna elements generates a narrow directional beam. Subsequently, the 2π angular area around the user is divided in S identical sectors of angular width equal to the half power beamwidth (HPBW) of the beam which is $2/N_U$ radians. In each sector, user transmit pilot symbols that are reflected by T_s tags falling within the sector. The user employs maximum likelihood estimator to estimate the ϕ_i of the reflected signals from T_s tags.

In the second phase, denoted by feedback phase, using sub-6 GHz control plane the user obtains unique identification number of each tag and then feedback the estimated angle $\hat{\phi}_i$ information to the respective tag. In the last phase, called optimization phase, each tag optimizes its $\boldsymbol{\Gamma}_i$ corresponding to the estimated $\hat{\phi}_i$ and ϕ'_i to direct the incident signal from AP to the user. Moreover, using information of estimated direction between user and tags, the user optimizes its beam steering direction to achieve maximum rate support. Thereafter, the data transmission phase begins.

IV. AoA Estimation

This section deals with estimation of AoA of the reflected signals from all the tags at the user. It is not possible to use a sub-spaced based algorithm since a ULA coupled to an RF unit only provides one measurement. Therefore, we propose employing an ML estimator to estimate $\{\phi_i\}_{\forall i}$ at the user equipped with a single RF chain.

We use ULA based geometry to design the tag reflection coefficient matrix $\boldsymbol{\Gamma}$ based only on angular information. Then, to reflect an incoming signal having incident angle ω_i to a direction an angle ω_r, the phase shift of the m^{th} reflecting element in $\boldsymbol{\Gamma}_i$ for i^{th} tag given as [8], [9]

$$\nu_{i,m}=(2\pi d'/\lambda_c)(m-1)(\sin\omega_i-\sin\omega_r). \tag{8}$$

During AoA estimation phase, all tags are assumed to be in a retro-reflective configuration, meaning that the angle of reflection at each tag is equal to the angle of incidence, i.e., $\omega_r=\omega_i$. As a result, the a signal transmitted by a user at an angle ϕ towards a tag is received back from the same direction, providing spatial filtering and thus, $\boldsymbol{\Gamma}_i=\zeta\mathbf{I}_{N_T}$. The user estimates the AoA from T tags by sequentially estimating AoA from T_s at a time that falls within a sector s, where $s=\{1,\ldots,S\}$. To estimate T_s AoAs in a sector s, the user sweeps each sector in L directions by varying its steering angle Ω in steps of Δ with the sector s, i.e.,

$$\Omega\in\left\{\frac{2(s-1)}{N_U}+\Delta,\ldots,\frac{2(s-1)}{N_U}+L\Delta\right\}\equiv\boldsymbol{\Omega} \tag{9}$$

where $\Delta=2\pi/2^b$. Here, b represents the number of quantization bits.

Let the user transmit same pilot signal x of power P over all N_c subcarriers through its beam steered at an angle $\Omega_l\in\boldsymbol{\Omega}$. Then the RF signal received at the antenna array of i^{th} tag is

$$\mathbf{y}_l[n]=\boldsymbol{H}_i[n]\boldsymbol{b}(\Omega_l)x. \tag{10}$$

Owing to channel reciprocity, the uplink channel between user and i^{th} tag is

$$\boldsymbol{H}'_i[n]=\sqrt{N_TN_U}h_i q(n,\tau_h)\mathbf{a}_{\mathrm{R}}(\phi_i)\mathbf{a}_{\mathrm{T}}^H(\phi_i)\in\mathbb{C}^{N_T\times N_U}. \tag{11}$$

Reflected signal from all tags are received by the user using the same beam steered at Ω_l. Therefore, the received signal is

$$\begin{aligned} y_l[n]=&\boldsymbol{b}^H(\Omega_l)\sum_{i=1}^{T_s}\boldsymbol{H}'_i[n]\boldsymbol{\Gamma}_i\boldsymbol{H}_i[n]\boldsymbol{b}(\Omega_l)x+z_l[n]\\ =&N_TN_U\boldsymbol{b}^H(\Omega_l)\left(\sum_{i=1}^{T_s}(h_i q(n,\tau_h))^2\mathbf{a}_{\mathrm{R}}(\phi_i)\mathbf{a}_{\mathrm{T}}^H(\phi_i)\boldsymbol{\Gamma}_i\right.\\ &\left.\times\,\mathbf{a}_{\mathrm{T}}(\phi_i)\mathbf{a}_{\mathrm{R}}^H(\phi_i)\boldsymbol{b}(\Omega_l)x\right)+z_l[n] \end{aligned} \tag{12}$$

where $z_l[n] \sim \mathcal{N}(0, \sigma^2)$. Since $\mathbf{\Gamma}_i = \zeta \mathbf{I}_{N_T}$, (12) reduces to

$$y_l[n] = N_T N_U \boldsymbol{b}^H(\Omega_l) \sum_{i=1}^{T_s} (h_i q(n, \tau_h))^2 \mathbf{a}_{\mathrm{R}}(\phi_i) \mathbf{a}_{\mathrm{R}}^H(\phi_i) \boldsymbol{b}(\Omega_l) x + z_l[n]. \tag{13}$$

It is notable that in (13) $\mathbf{a}_{\mathrm{R}}(\phi_i) = \mathbf{a}(\phi_i)_{N=N_U}$. Further, let $\beta_i[n] = N_T N_U (h_i q(n, \tau_h))^2$ and $\boldsymbol{\beta}[n] = [\beta_1[n], \dots \beta_{T_s}[n]]^T$. Then

$$\begin{aligned} y_l[n] &= \sum_{i=1}^{T_s} \boldsymbol{b}^H(\Omega_l) \mathbf{a}(\phi_i) \mathbf{a}^H(\phi_i) \boldsymbol{b}(\Omega_l) \beta_i[n] x + z_l[n] \\ &= (\boldsymbol{b}^H(\Omega_l) \mathbf{A} \odot (\mathbf{A}^H \boldsymbol{b}(\Omega_l)^T) \boldsymbol{\beta}[n] x + z_l[n]. \end{aligned} \tag{14}$$

Here $\mathbf{A} = [\mathbf{a}(\phi_1), \dots \mathbf{a}(\phi_{T_s})] \in \mathbb{C}^{N_U \times T_s}$ and $\odot$ denotes element wise product. Let $\bar{\boldsymbol{\beta}} = \{\boldsymbol{\beta}[1], \dots, \boldsymbol{\beta}[N_c]\} \in \mathbb{C}^{T_s \times N_c}$. Then the received signal vector over all subcarriers is

$$\mathbf{y}_l = (\boldsymbol{b}^H(\Omega_l) \mathbf{A} \odot (\mathbf{A}^H \boldsymbol{b}(\Omega_l))^T) \bar{\boldsymbol{\beta}} x + \mathbf{z}_l \in \mathbb{C}^{1 \times N_c}. \tag{15}$$

Over all L steering directions in a sector sweep, the received signal is

$$\mathbf{Y} = (\boldsymbol{B}^H \mathbf{A} \odot (\mathbf{A}^H \boldsymbol{B})^T) \bar{\boldsymbol{\beta}} x + \mathbf{Z} \in \mathbb{C}^{L \times N_c} \equiv \bar{\mathbf{D}} \bar{\boldsymbol{\beta}} + \mathbf{Z} \tag{16}$$

where $\boldsymbol{B} = [\mathbf{b}(\Omega_1), \dots \mathbf{b}(\Omega_L)] \in \mathbb{C}^{N_U \times L}$ and $\mathbf{Z} \in \mathbb{C}^{L \times N_c}$ is the noise matrix. (16) is the sum of reflected signals coming from only a small number of directions. Hence, the solution to AoA estimation at the user is sparse. Therefore, in each sector s, we employ ML estimator to recover T_s directions of arrival $\{\phi_i\}$. Let $\boldsymbol{\phi} = \{\phi_1, \dots, \phi_{T_s}\}$, then the ML estimator for sector s is represented as

$$\begin{aligned} (\mathcal{P}1) : &\underset{\boldsymbol{\phi}}{\operatorname{argmin}} \ \|\mathbf{Y} - \mathbf{D}\mathbf{D}^\dagger \mathbf{Y}\|^2 \\ &\text{s.t. } 2(s-1)/N_U \le \phi_i \le 2s/N_U \ \forall i = \{1, \dots, T_s\}. \end{aligned} \tag{17}$$

Here, $\mathbf{D}^\dagger$ represents Moore–Penrose inverse of a matrix $\mathbf{D}$. Each column of dictionary matrix $\mathbf{D} \in \mathbb{C}^{L \times T_s}$ is given as

$$\mathbf{d}(\phi) = \boldsymbol{B}^H \mathbf{a}(\phi) \odot (\mathbf{a}^H(\phi) \boldsymbol{B})^T. \tag{18}$$

Problem $(\mathcal{P}1)$ is non-convex. Therefore, we find local minima around an initial estimate. We procure the initial estimate of AoAs using OMP estimator [10]. For analytically simplicity, we assume that the number of tags falling within the beam's coverage area T_s is known a priori. The steps of the OMP estimator are given in Algorithm 1.

Algorithm 1 OMP

Input: $i = 0$, $\mathbf{r}_i = \mathbf{Y}$, $\mathbf{d}(\phi)$, $\delta = 0.001$
Output: $\{\phi_1, \dots \phi_{T_s}\}$
Initialize
do
  $\phi^* = \underset{\phi \in \Phi}{\operatorname{argmax}} \|\mathbf{d}(\phi)^H \mathbf{r}_i\|$
  Update $\phi_e = \phi_e \cup \phi^*$
  Increment i
  $\mathbf{Q} = \mathbf{d}(\phi_e)\mathbf{d}(\phi_e)^H \mathbf{d}(\phi_e))^{-1} \mathbf{d}(\phi_e)^H$
  $\mathbf{r}_i = (\mathbf{I} - \mathbf{Q})\mathbf{Y}$
while $i \le T_s$ and $\mathbf{r}_i \ge \epsilon$

Therefore, from (8), the m^{th} optimal reflecting coefficient of i^{th} tag is given as

$$\nu_{i,m}^* = (2\pi d'/\lambda_c)(m-1)(\sin \phi_i' - \sin \hat{\phi}_i) \tag{19}$$

where $\hat{\phi}_i$ is the estimated AoA at user from i^{th} tag.

A. Cramer-Rao Bound Analysis

Next, we derive the lower bound on the AoA estimation using Cramer-Rao bound. From (14), the received signal over I snapshots on n^{th} subcarrier within a sector s is

$$\boldsymbol{y}[n] = \boldsymbol{\mu}[n] + \boldsymbol{z}[n] \tag{20}$$

where $\boldsymbol{\mu}[n]$ denotes the noiseless part of received signal. Let the vector of unknown parameters in (20) over a subcarrier n is given by $\boldsymbol{\eta} = [\boldsymbol{\phi}, Re\{\boldsymbol{\beta}\}, Im\{\boldsymbol{\beta}\}] \in \mathbb{C}^{3T_s \times 1}$.

Subsequently, for I snapshots, the Fisher information matrix (FIM) $\boldsymbol{J}(\boldsymbol{\eta}) \in \mathbb{R}^{3T_s \times 3T_s}$ for s^{th} sector is defined as [11]

$$\boldsymbol{J}(\boldsymbol{\eta}) = \frac{2}{\sigma^2} \sum_{i=1}^{I} \sum_{n=1}^{N_c} Re \left\{ \frac{\partial [\boldsymbol{\mu}[n]]_i}{\partial \boldsymbol{\eta}} \left(\frac{\partial [\boldsymbol{\mu}[n]]_i}{\partial \boldsymbol{\eta}} \right)^H \right\} \tag{21}$$

where

$$\begin{aligned} \frac{\partial [\mu_l[n]]_i}{\partial \phi_k} &= -j \frac{2\pi d'}{\lambda_c} \frac{\beta_k[n] \cos \phi_k}{N_U N_U} \times \\ &\quad \sum_{n=1}^{N_u} \sum_{m=1}^{N_u} (m-n) e^{-\frac{j2\pi d'}{\lambda_c}(m-n)(\sin \phi_i - \sin \Omega_l)} x \\ \frac{\partial [\boldsymbol{\mu}[n]]_i}{\partial Re(\beta_k[n])} &= (\boldsymbol{B}^H \mathbf{a}(\phi) \odot \boldsymbol{B}^H \mathbf{a}(\phi)) x \\ \frac{\partial [\boldsymbol{\mu}[n]]_i}{\partial Im(\beta_k[n])} &= j(\boldsymbol{B}^H \mathbf{a}(\phi) \odot \boldsymbol{B}^H \mathbf{a}(\phi)) x. \end{aligned} \tag{22}$$

Using (21), the Angle Error Bound (AEB) of ϕ_k is

$$\text{AEB} = \sqrt{\text{diag}[\mathbf{J}^{-1}(\boldsymbol{\eta})]_{k,k}}. \tag{23}$$

Thus, AEB is the lower bound on ϕ_k estimate.

V. Steering vector optimization

Following AoA estimation at the user and optimization of tag reflection coefficients, in this section we optimize the user's analog combiner. Since a user has one RF unit connected to a ULA, optimizing the analog combiner is equivalent to determining the best steering direction. Below we describe the various schemes for optimizing user steering direction.

- Sectoring scheme: As discussed in Section IV, area around the user is divided into S sectors. So, a codebook is made up of fixed steering vectors corresponding to steering angles in $\boldsymbol{\Omega}_S = \{(2s-1)/N_U | s = \{1, \dots, S\}\}$ radian. Then, the optimal user steering angle is $\Omega^* = \underset{\Omega \in \boldsymbol{\Omega}_S}{\operatorname{argmax}} \ R(\Omega)$, where $R(\Omega)$ denotes the rate achieved by user when its beam is steered at direction Ω.
- Grouping scheme: The tags are grouped using k-means clustering. Given N_U, the number of clusters is equal

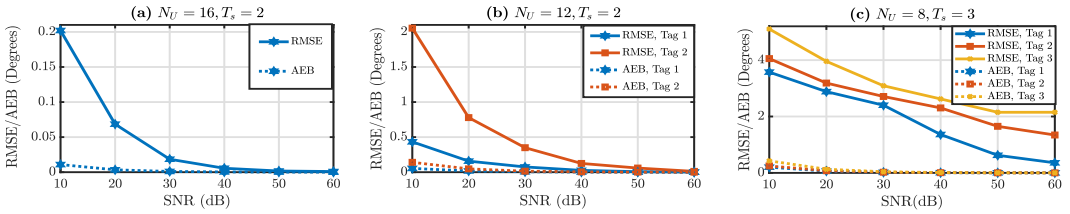

Figure 2: RMSE and AEB of proposed AoA estimator.

to the number of sectors with at least one tag i.e, $k = \sum_{s=1}^{|\Omega_S|} \pi_s$ where $\pi_s = 1$ if $T_s \geq 1$; 0 otherwise. Further, the steering angle Ω_g of the g^{th} cluster is equal to the median of all the AoAs in group g. Therefore, the set of steering angles is $\mathbf{\Omega}_G = \{\Omega_g | g = \{1, \ldots, k\}\}$. Consequently, optimal user steering direction is $\Omega^* = \underset{\Omega \in \mathbf{\Omega}_G}{\text{argmax}}\ R(\Omega)$.

- Exhaustive scheme: This scheme is similar to sectoring except that there are E scanning directions separated by $\delta\phi = 2\pi/E$ radian intervals regardless of beamwidth. Therefore, the set of all steering directions in the codebook is $\mathbf{\Omega}_E = \{0, \delta\phi, \ldots, (E-1)\delta\phi\}$. The optimal beam direction at user is the found as $\Omega^* = \underset{\Omega \in \mathbf{\Omega}_E}{\text{argmax}}\ R(\Omega)$.

VI. Results and Discussions

In this section, we present the numerical results obtained from MATLAB Monte Carlo simulations. Table I lists the values of various simulation parameters used. In addition, we use the thinning method to simulate the non-homogeneous tag distribution, with thinning intensity equal to 3.

Fig. 2 shows the root mean squared error (RMSE) of the proposed AoA estimator and compares it to the AEB for various N_U values. Notably, a higher value of N_U results in a narrower beam, reducing the effective number of tags and hence total number of reflecting elements $\bar{N}_T$ that contribute to virtual paths between the AP and the user, as shown in Fig. 3. As illustrated in Fig. 2(a), with $N_U = 16$ and $\lambda = 1$ tags/m^2, only one tag falls within a sector on average, and the RMSE reaches the AEB at high signal-to-noise (SNR) values. The average number of tags per sector increases to two and three when $N_U = 12$ and $N_U = 8$, respectively. Subsequently, the RMSE also increases, as shown in Fig. 2(b)

Table I: Simulation parameters

Parameter	Variable	Value
Length of room	L	5m
Width of room	W	10 m
Carrier frequency	f_c	28 GHz
Number of subcarriers	N_c	30
Bandwidth	B	100 MHz
Bits	b	10
Rician fading parameter	κ	18 dB
Noise power spectral density	N_0	-174 dbm/Hz/s
Reflection amplitude attenuation	ζ	0.5
Number of reflecting elements at tag	N_T	8
Number of antenna elements at AP	N_{AP}	4
Wall tip 2D coordinates	$[x_W, y_W]$	$[1.44, L/2]$ m
AP 2D coordinates	$[x_{AP}, y_{AP}]$	$[0, L]$ m
RIS 2D coordinates	$[x_R, y_R]$	$[W/2, L/2]$ m
AP transmit power	P	33 dBm [12]

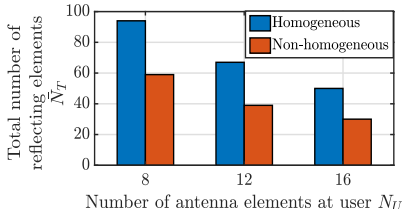

Figure 3: Average number of reflecting elements $\bar{N}_T$ aiding AP to user communication when tags are distributed homogeneously and non-homogeneously with $\lambda = 2$ and $N_T = 8$.

and Fig. 2(c). There are two reasons for the increase in RMSE. First, the correlation in the OMP algorithm decreases as the number of closely located tags T_s increases. Furthermore, OMP is a residue-based algorithm. Therefore, the error in initial AoA estimate of first tag propagates into the initial AoA estimate of second tag, and so on. Moreover, because the ML estimator is non-convex, we can only find local minimums near the initial points. As a result, the output of ML estimator is affected by the initial AoA estimates obtained from OMP algorithm. Fig. 4 illustrates the reduction in rate at the user when using erroneous estimated AoAs to design tags' reflection coefficients and combiner at user as compared to using exact AoAs.

Following that, we compare the data rate obtained with tags for three different user beam steering strategies discussed in Section V. We also compare the results to those obtained when a fixed linear RIS is used to assist the communication between the AP and blocked user. Since the location of user is unknown hence, in simulation we consider RIS coordinates as $[W/2, L/2]$ to provide coverage at all points behind the wall. For a fair comparison, we take the number of reflecting elements at RIS to be equal to $\bar{N}_T$. Additionally, we compare the results with another scheme in which the tags have random $\mathbf{\Gamma}_i$ and user beam sweeps the area in a round-robin fashion. As a result, no initial angle estimation, feedback, or reflection coefficient optimization are required.

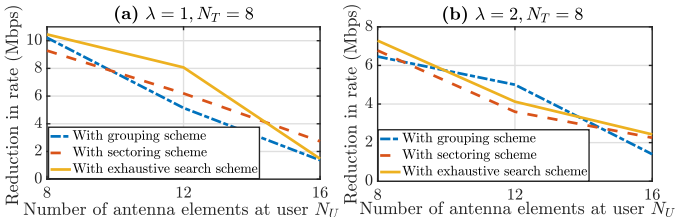

Figure 4: Reduction in rate when using estimated AoAs as compared to using true AoAs to design tags' reflection coefficients and user steering direction in case of homogeneously distributed tags.

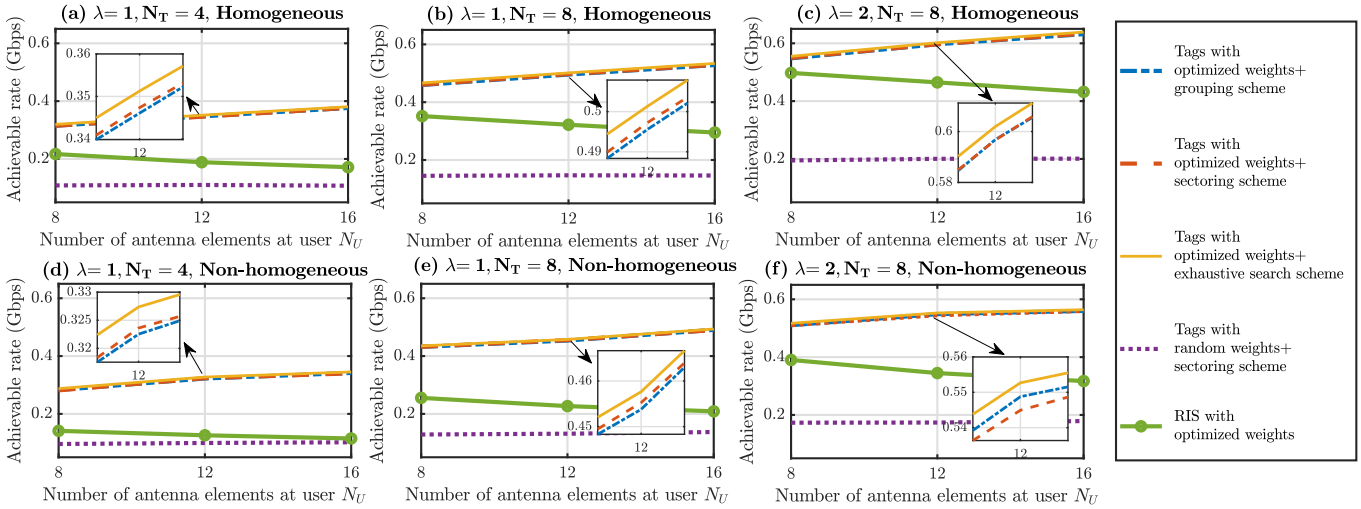

Figure 5: Comparison of achievable rate with different schemes for homogeneously distributed and non-homogeneously distributed tags.

Fig. 5 depicts the rate achieved with different schemes for different simulation scenarios. As illustrated, the achievable rate with sectoring, grouping and exhaustive search schemes improves with N_U despite the fact that average number of reflecting elements $\bar{N}_T$ decreases as N_U increases. This is because of higher array gain at user and lower RMSE of the AoA estimator at higher value of N_U. Moreover, Fig. 5, shows that using tags distributed over an area gives better rate support than using a single RIS with having $\bar{N}_T$ number of relfecting elements. Further, at high value of N_U and small value of $\bar{N}_T$, rate achieved by using random weights at tags approaches the rate achieved using RIS, as shown in Fig. 5(a) and Fig. 5(d).

VII. Conclusion

In this paper, we proposed utilizing existing backscatter infrastructure to provide connectivity to a blocked user with unknown coordinates in an indoor mmWave communication system. First, by configuring the tags in retro-reflective mode, we proposed a novel method for estimating the AoA from tags to the user. Following that, a joint OMP and ML estimator is proposed to estimate the AoAs at the user equipped with a single RF chain. It was observed that at a sufficiently high SNR and a large number of antenna elements at the user, the estimator's RMSE reaches AEB. This condition deteriorates with decreasing ULA size of the user. Furthermore, the user steering direction and tag weights are optimized to maximize the user's achievable rate. The findings demonstrated that the existing backscatter infrastructure can support mmWave communications while providing improved gains over that achieved using a single RIS with an equivalent number of reflecting elements as at the tags. Although few tags contributes to the less number of paths between AP and user, a narrow beam of high gain nevertheless achieves a higher gain in both homogeneous and non-homogeneous tag distribution cases.

VIII. Acknowledgment

This work was supported in part by the Academy of Finland project BESMIAL (grant no: 334197); in part by the Science and Engineering Board, Department of Science and Technology (DST), Government of India, under Grant CRG/2019/002293; in part by the Indian National Academy of Engineering (INAE) through the Abdul Kalam Technology Innovation National Fellowship; and in part by the MediaTek Research Fellowship (FT/2022/11/9).

References

[1] N. Varshney and S. De, "Optimum downlink beamwidth estimation in mmWave communications," *IEEE Trans. Commun.*, vol. 69, no. 1, pp. 544–557, 2020.

[2] Z. Li, H. Hu, J. Zhang, and J. Zhang, "Enhancing indoor mmwave wireless coverage: Small-cell densification or reconfigurable intelligent surfaces deployment?" *IEEE Wireless Commun. Lett.*, vol. 10, no. 11, pp. 2547–2551, 2021.

[3] M. Naderi Soorki, W. Saad, M. Bennis, and C. S. Hong, "Ultra-reliable indoor millimeter wave communications using multiple artificial intelligence-powered intelligent surfaces," *IEEE Tran. Commun.*, vol. 69, no. 11, pp. 7444–7457, 2021.

[4] A. Al-Nahari, R. Jantti, and M. U. Sheikh, "Artificial rich scattering-assisted mimo systems using passive backscatter devices," in *3rd Information Commun. Technol. Conf. (ICTC)*, 2022, pp. 19–24.

[5] J. Kimionis, A. Georgiadis, S. N. Daskalakis, and M. M. Tentzeris, "A printed millimetre-wave modulator and antenna array for backscatter communications at gigabit data rates," *Nature Electronics*, vol. 4, no. 6, pp. 439–446, 2021.

[6] B. Zheng, C. You, W. Mei, and R. Zhang, "A survey on channel estimation and practical passive beamforming design for intelligent reflecting surface aided wireless communications," *IEEE Commun. Surveys & Tut.*, vol. 24, no. 2, pp. 1035–1071, 2022.

[7] M. McCloud and L. Scharf, "A new subspace identification algorithm for high-resolution doa estimation," *IEEE Trans. Antennas and Propagation*, vol. 50, no. 10, pp. 1382–1390, 2002.

[8] E. Soltanaghaei, A. Prabhakara, A. Balanuta, M. Anderson, J. M. Rabaey, S. Kumar, and A. Rowe, "Millimetro: mmwave retro-reflective tags for accurate, long range localization," in *Proc. 27th Annual Int. Conf. Mobile Computing and Networking*, 2021, pp. 69–82.

[9] M. H. Mazaheri, A. Chen, and O. Abari, "mmtag: a millimeter wave backscatter network," in *Proc. ACM SIGCOMM 2021 Conference*, 2021, pp. 463–474.

[10] T. T. Cai and L. Wang, "Orthogonal matching pursuit for sparse signal recovery with noise," *IEEE Trans. Information theory*, vol. 57, no. 7, pp. 4680–4688, 2011.

[11] S. M. Kay, *Fundamentals of statistical signal processing: Estimation theory*. Prentice-Hall, Inc., 1993.

[12] 3GPP. (2018) 5G NR; User Equipment (UE) radio transmission and reception; Part 2: Range 2 Standalone, Rel-15. 3GPP TS 38.101-2 V15.2.0.